Intercalation of (η^5-pentamethylcyclopentadienyl)trioxo-molybdenum(VI) in a layered double hydroxide

Ana C. Gomes,[a] Patrícia Neves,[a] Sandra Gago,[a][‡] Anabela A. Valente,*[a] Isabel S. Gonçalves,[a] and Martyn Pillinger*[a]

Abstract: A Zn,Al layered double hydroxide (LDH) with [Cp*MoO$_3$]$^-$ (Cp* = η^5-C$_5$Me$_5$) anions in the interlayer has been prepared by a direct coprecipitation method. The intercalated LDH and the mixed metal oxide (MMO) obtained after its calcination were characterized by elemental and thermogravimetric analyses, powder X-ray diffraction (PXRD), FT-IR and FT-Raman spectroscopies, ^{13}C and ^{27}Al MAS NMR, and scanning electron microscopy. The observed basal spacing of 17.1 Å for the LDH Zn,Al-Cp*MoO$_3$ (corresponding to a gallery height of 12.3 Å) suggests that the guest anions self-assemble into dimers via offset face-to-face Cp*···Cp* interactions, which facilitates hydrogen-bonding interactions between the oxido ligands of the complexes and the layer hydroxyl groups, while positioning the hydrophobic aromatic rings towards the center of the galleries. Calcination of Zn,Al-Cp*MoO$_3$ at 550 °C under air gave an MMO comprising well-dispersed ZnO, α-ZnMoO$_4$ and ZnAl$_2$O$_4$ (spinel) oxides in a molar of *ca.* 1.4:1.6:1. The MMO exhibited catalytic activity for the epoxidation of *cis*-cyclooctene with *tert*-butylhydroperoxide (TBHP) as terminal oxidant, with quantitative yield of the epoxide being achieved within 24 h at 85 °C.

Introduction

The intercalation of atomic or molecular guest species into lamellar inorganic crystals has been explored since the 1970s as a means to engineer complex organized structures at the nanoscale.[1-5] Intercalation can modify the physical and chemical properties of the host and guest, leading to new materials with optical, optoelectronic, conductive, energy storage, and catalytic applications, among others. Two-dimensional (2D) layered materials provide the structural flexibility needed to carry out these reactions since the weakly interacting host layers can be separated by large distances (up to 50 Å) to accommodate bulky guests in the interlamellar region. Research on the intercalation of organometallic guest molecules into inorganic layered host matrices[5] was kickstarted by Dines with the intercalation of cobaltocene (CoCp$_2$, Cp = η^5-C$_5$H$_5$) into metal dichalcogenides MX$_2$ (M = Ti, Zr, Nb, Ta and Sn; X = S, Se).[6] Since then a large number of bis-Cp and bis-arene sandwich complexes (and their ring-substituted derivatives) and bent metallocenes such as Cp$_2$MoCl$_2$ have been intercalated into a range of host lattices including metal dichalcogenides,[7-10] MOCl (M = Fe, V, Ti),[11] MPS$_3$ (M = Mn, Zn, Fe, Ni),[12] β-ZrNCl,[13] MoO$_3$,[14] zirconium phosphate,[14-17] vanadyl phosphate,[18,19] layered silicates,[20,21] and layered double hydroxides (LDHs).[22-27] In sharp contrast, there are few reports of the incorporation of half-sandwich "piano stool" complexes within inorganic layered materials, with two examples being [CpRu(benzo-15-crown-5)]$^+$ in MPS$_3$ (M = Mn, Cd, Zn),[28] and [CpMo(CO)$_3$CH$_2$COO$^-$] in a Zn,Al LDH.[29]

LDHs are unusual among intercalation hosts in that they possess positively charged layers with exchangeable interlayer anions.[30] This anion-exchange behavior, coupled with their low cost, ease of synthesis, and high compositional flexibility, makes LDHs ideally suited to the production of hybrid materials that combine an extended inorganic framework with an ordered molecular array.[31-33] These hybrid materials can be obtained not only by anion exchange but also by direct self-assembly (coprecipitation) methods involving the *in situ* formation of LDHs around the guest molecules, which may act as templates. The positive charge of LDH layers arises from the presence of trivalent metal ions M^{3+} (*e.g.*, Al^{3+}, Fe^{3+}, Ga^{3+}, Cr^{3+}) in addition to divalent metal ions M^{2+} (*e.g.*, Mg^{2+}, Fe^{2+}, Ni^{2+}, Zn^{2+}) in brucite (Mg(OH)$_2$)-like layers built up from edge-sharing M(OH)$_6$ octahedra. The positive charge is balanced by anions (A^{m-}) weakly bonded by electrostatic forces and placed in the interlayers conjointly with water molecules. The general formula can be written as [M$^{2+}_{1-x}$M$^{3+}_x$(OH)$_2$]$^{x+}$(A^{m-})$_{x/m}$·nH$_2$O.

Despite the work on the preparation of LDHs containing a plethora of different anions, only a few reports describe the incorporation of η^5-cyclopentadienyl metal complexes. Apart from the half-sandwich molybdenum tricarbonyl complex mentioned above, the published studies concern anionic ferrocene derivatives containing carboxylate,[22,23] sulfonate,[23-25] butyrate,[26] and alkylsulfonate[27] substituent groups.

In this paper we report the direct self-assembly synthesis of an expanded LDH intercalated phase containing the trioxido anion [Cp*MoO$_3$]$^-$ (Cp* = η^5-C$_5$Me$_5$). In addition, we present an exhaustive characterization of the inorganic/organometallic nanomaterial that allows a plausible structural model to be proposed for the highly ordered packing arrangement of guest molecules. The thermal stability of the material has been studied and catalytic results are presented for a mixed metal oxide (MMO) composite prepared by thermal treatment.

Results and Discussion

Synthesis and characterization

The anion [Cp*MoO$_3$]$^-$ was isolated as its sodium salt by oxidation of Na[Cp*Mo(CO)$_3$] with six equivalents of TBHP under basic conditions. Ion-exchange and direct synthesis methods were explored to prepare a Zn,Al LDH intercalated by the

[a]   Dr. A.C. Gomes, Dr. P. Neves, Dr. S. Gago, Dr. A.A. Valente, Prof.
Dr. I.S. Gonçalves, Dr. M. Pillinger
*CICECO - Aveiro Institute of Materials, Department of Chemistry,
University of Aveiro, Campus Universitário de Santiago, 3810-193
Aveiro, Portugal*
E-mail: atav@ua.pt (A.A.V.)
Homepage: http://www.ciceco.ua.pt/AnabelaValente
E-mail: mpillinger@ua.pt (M.P.)
*Homepage: http://www.ciceco.ua.pt/MartynPillinger*

[‡]   *Present address: LAQV-REQUIMTE, Departamento de Química,
Faculdade de Ciências e Tecnologia, Universidade NOVA de
Lisboa, 2829-516 Caparica, Portugal*

trioxido complex. The ion exchange approach, using a Zn,Al-NO$_3$ precursor and excess Na[Cp*MoO$_3$] dissolved in either water or a THF/MeOH mixture, did not lead to any significant intercalation after stirring the mixture at 50 °C for two days, as evidenced by FT-IR spectroscopy and PXRD. This method was therefore abandoned and the direct coprecipitation method was pursued, which has previously been used to prepare LDHs intercalated by ferrocene(di)carboxylate anions[22] and the half-sandwich complex [CpMo(CO)$_3$CH$_2$COO$^-$].[29] The trioxido anion [Cp*MoO$_3$]$^-$ is compatible with this synthesis strategy since it is stable in neutral to mildly alkaline aqueous solutions. In the optimized procedure, an aqueous solution containing Zn(NO$_3$)$_2$ (50 mM) and Al(NO$_3$)$_3$ (25 mM) was added dropwise to a solution of Na[Cp*MoO$_3$] (in a 2-fold excess over that theoretically required), and the pH of the mixture was maintained between 7.5 and 8 by dropwise addition of dilute NaOH. After aging the resultant gel-like slurry at 65 °C for 20 h, a pale yellow solid (denoted as Zn,Al-Cp*MoO$_3$) was recovered.

The PXRD pattern of Zn,Al-Cp*MoO$_3$ is shown in Figure 1. Five quite sharp, symmetric and equally spaced peaks between 3 and 30° 2θ are assigned as the (00l) reflections of a hydrotalcite-type LDH phase with a basal spacing ($d_{(003)}$) of 17.1 Å. Subtraction of 4.8 Å for the layer thickness gives a gallery height of 12.3 Å. The crystal structure of Na[Cp*MoO$_3$]·5H$_2$O was determined by Dinoi et $al.$[34] Visualizing the trioxido anion as a three-legged piano-stool, its van der Waals (vdW) molecular dimensions are a width of $ca.$ 8.6 Å (corresponding to the diameter of the Cp* ligand) and a height of $ca.$ 6.4 Å. The gallery height of Zn,Al-Cp*MoO$_3$ therefore suggests the presence of a bilayer of intercalated [Cp*MoO$_3$]$^-$ anions rather than a monolayer. A bilayer arrangement is expected since the trioxido anion would not be spatially capable of compensating the host layer positive charge if arranged in a monolayer. Specifically, the area per unit positive charge of an LDH with the general formula [Zn$_{1-x}$Al$_x$(OH)$_2$]$^{x+}$ is given by $(1/x)a_o^2\sin60°$, where a_o is the hexagonal unit cell parameter. This means that for a Zn,Al LDH with x = 0.33 and a_o ~ 3.1 Å, a monolayer of intercalated monovalent anions can be formed if their cross-sectional area is less than 25 Å. Two important vdW cross-sectional areas can be estimated for the trioxo anion: 53.0 Å^2 for the view perpendicular to the plane formed by the Cp* ring, and 44.5 Å^2 for the view perpendicular to the Mo-Cp*(centroid) axis. These estimates indicate that a bilayer of densely packed trioxido anions could almost fully balance the layer charge of a Zn$_2$Al-LDH.

The relative intensities of the (00l) reflections in the PXRD pattern of Zn,Al-Cp*MoO$_3$ provide additional support for the present of a bilayer of guest anions. The key feature is the alternation of the intensities according to the sequence (003) > (006) < (009) > (0012). This fluctuation in (00l) intensities is known to occur when there is an increase in the electron density in the interlayers due to the presence of molecular species containing heavy metals. The specific sequence observed for Zn,Al-Cp*MoO$_3$ is symptomatic of a bilayer arrangement and has been observed previously for Zn,Al LDHs intercalated by ferrocenecarboxylate and [CpMo(CO)$_3$CH$_2$COO$^-$] anions.[22,29] An opposite intensity sequence, $i.e.$ (003) < (006) > (009) <

(0012), indicates the presence of a monolayer of guest species, $i.e.$ a high concentration of electron density in the midplane ($d_{(003)}$/2) of the interlayer region, and has been observed previously for LDHs intercalated by, for example, 1,1'-ferrocenedicarboxylate,[22] cis-[Mo(CO)$_4$(bpdc)]$^{2-}$ (bpdc = 2,2'-bipyridine-5,5'-dicarboxylate),[35] mixed ligand platinum complexes [PtCl$_{(6-x)}$(OH)$_x$]$^{2-}$,[36] and the chromium oxalate complex [Cr(C$_2$O$_4$)$_3$]$^{3-}$.[37]
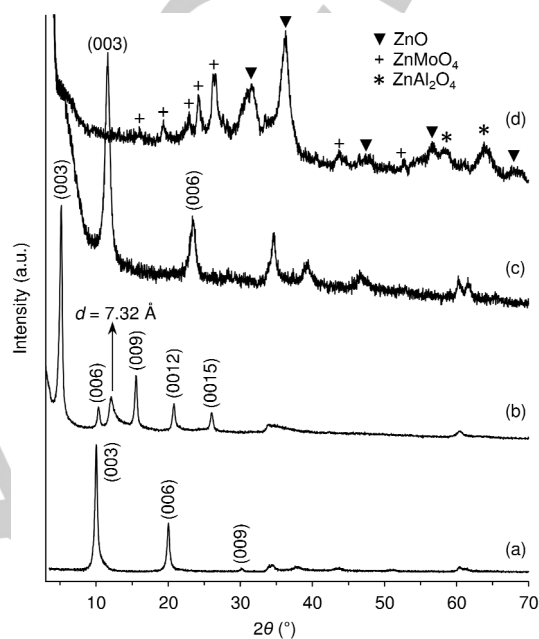

Figure 1. PXRD patterns of (a) Zn,Al-NO$_3$, (b) Zn,Al-Cp*MoO$_3$, (c) Zn,Al-exCO$_3$, and (d) calZn,Al-Cp*MoO$_3$.

The PXRD pattern of Zn,Al-Cp*MoO$_3$ contains a broader, somewhat asymmetric peak at 12.07° 2θ (7.32 Å). An experiment was performed in which the guest interlayer species in Zn,Al-Cp*MoO$_3$ were fully exchanged with carbonate anions, giving the material denoted as Zn,Al-exCO$_3$. The PXRD pattern of Zn,Al-exCO$_3$ is typical of Zn,Al-CO$_3$ LDHs, showing a $d_{(003)}$ spacing of 7.62 Å (Figure 1). Neither the peak at 7.32 Å nor the (00l) reflections for Zn,Al-Cp*MoO$_3$ are observed in the pattern of the carbonate-exchanged material. We therefore attribute the asymmetric peak to anion ordering rather than an impurity phase. Although it is quite rare for PXRD to reveal evidence for anion ordering in LDHs, anomalous peaks in the diffraction patterns of some organic-anion-intercalated LDHs have been attributed to a highly regular distribution of guest species.[30,38,39] The previously mentioned Zn,Al LDH intercalated by [CpMo(CO)$_3$CH$_2$COO$^-$] anions also gave a diffraction pattern containing an anomalous peak (at 6.37 Å), which again was attributed to guest ordering since carbonate exchange promoted the loss of this peak in addition to the basal reflections of the organometallic-anion-intercalated phase.[29]

From the above considerations we may conclude that the trioxido anions in the material Zn,Al-Cp*MoO$_3$ are closely packed and that this dense arrangement results in an ordered

distribution of Mo centers. The crystal structure of Na[Cp*MoO$_3$]·5H$_2$O provides some insight into how the trioxido anions may be arranged in the intercalated LDH.[34] Thus, the anions in the sodium salt assemble to form two distinct pairs (P1 and P2) that feature a parallel offset face-to-face π-stacking of the Cp* rings. One of the pairs has a perpendicular interplanar distance of 3.68 Å and an offset of 0.8 Å, while the other pair displays a higher displacement of 3.5 Å and a shorter interplanar distance of 3.50 Å. Infinite rows of pairs P1 and P2 (down the crystallographic *a* axis) alternate along the *b* axis to form a 2D supramolecular array. The three shortest Mo···Mo distances are 6.985, 7.240 and 7.663 Å, which span the *d*-spacing of the anomalous peak observed in the diffraction pattern of Zn,Al-Cp*MoO$_3$. The 2D arrays of organometallic anions in Na[Cp*MoO$_3$]·5H$_2$O are separated from each other by a 2D array of sodium ions and water molecules comprising individual [Na$_4$(H$_2$O)$_{16}$]$^{4+}$ clusters. The anion layers are connected to the cation layers by hydrogen bonds between the oxido groups of Mo^{VI} complexes and both free and Na$^+$-coordinated water molecules. Several of these structural features are likely to be present in Zn,Al-Cp*MoO$_3$, namely association of organometallic anions to form pairs via face-to-face π-stacking, and interaction of the anions with the cationic layers via O···HO hydrogen bonds. The vdW length of P1 (*i.e.* in a direction perpendicular to the plane of the Cp* rings) is 12.3 Å, which exactly matches the value of the gallery height determined by PXRD (the corresponding distance for P2 is 12.1 Å). Hence, the simplest structural model for intercalated trioxido complexes in Zn,Al-Cp*MoO$_3$ that is consistent with both the PXRD data and the anticipated packing arrangement comprises P1 pairs oriented to form a bilayer of Mo atoms (Figure 2). This arrangement facilitates H-bonding interactions between the oxido ligands of the complexes and the layer hydroxyl groups, while positioning the hydrophobic aromatic rings towards the center of the galleries, permitting π-π stacking interactions between the Cp* ligands of complexes in the upper and lower layers.
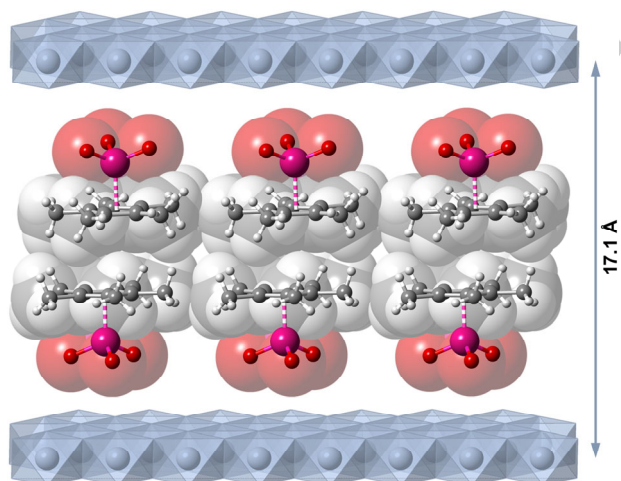
Figure 2. Structural model for the bilayer arrangement of [Cp*MoO$_3$]$^-$ anions in the material Zn,Al-Cp*MoO$_3$. The P1 pair of face-to-face stacked complexes was extracted from the crystal structure of Na[Cp*MoO$_3$]·5H$_2$O.[34]
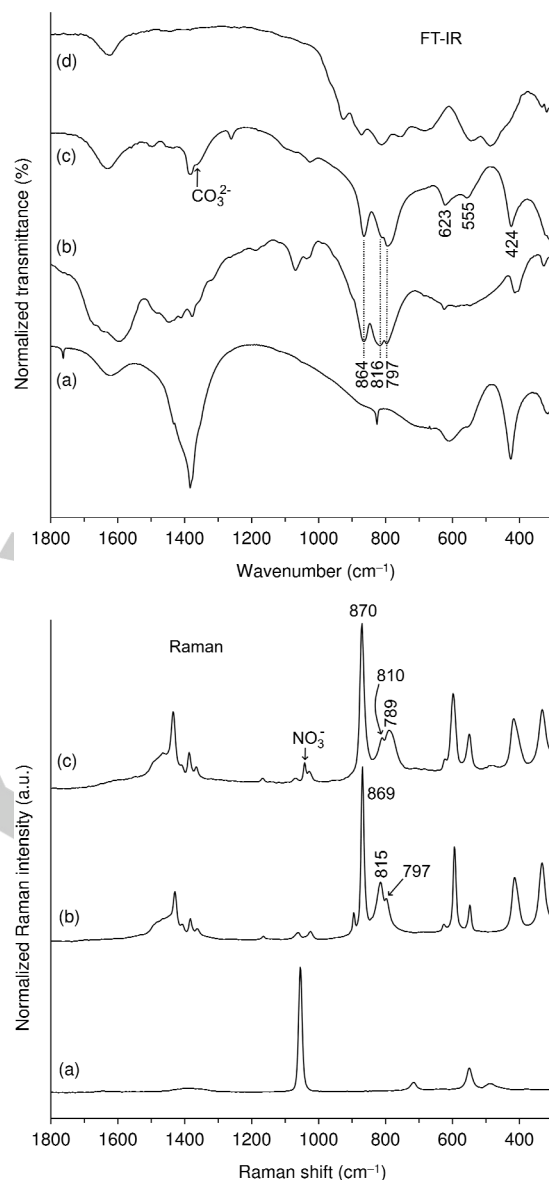
Figure 3. FT-IR and Raman spectra in the range 300-1800 cm^{-1} for (a) Zn,Al-NO$_3$, (b) Na[Cp*MoO$_3$]·2.5H$_2$O, (c) Zn,Al-Cp*MoO$_3$, and (FT-IR only) (d) calZn,Al-Cp*MoO$_3$. The positions of selected bands are indicated.

In the carbonate-exchange experiment mentioned above, the pale yellow solution recovered after ion-exchange was evaporated to dryness to give a pale yellow solid. The ^{1}H NMR spectrum of this solid in D$_2$O displayed a single sharp resonance (singlet) at 1.90 ppm, which is in exact agreement with the methyl group resonance displayed by Na[Cp*MoO$_3$] in D$_2$O. This result indicates that no Cp*-derived species other than [Cp*MoO$_3$]$^-$ anions were present in the material Zn,Al-Cp*MoO$_3$.

FT-IR, FT-Raman and ^{13}C{^{1}H} CP MAS NMR spectra were obtained for Zn,Al-Cp*MoO$_3$ to confirm the successful intercalation of [Cp*MoO$_3$]$^-$ anions. Most of the characteristic IR and Raman bands of the trioxido complex are present in the spectra of Zn,Al-Cp*MoO$_3$ (Figure 3). The IR/Raman bands

recorded at 864/870 and 812/810 cm⁻¹ for the intercalated LDH are assigned to the symmetric and asymmetric Mo–O stretching vibrations of the (MoO_3) moiety, respectively,[40] and appear at positions very close to those of the free complex. Below 700 cm⁻¹, the three main bands observed at 424, 555 and 623 cm⁻¹ in the IR spectrum of Zn,Al-Cp*MoO₃ are attributed to the characteristic Zn/Al-OH lattice translation modes of Zn,Al LDHs[41]; similar bands are observed for the nitrate-form material Zn,Al-NO₃. In the range 300-700 cm⁻¹, the Raman spectrum of Zn,Al-Cp*MoO₃ is dominated by bands due to the organometallic guest (at 332, 417, 549 and 598 cm⁻¹), and only a weak and broad band at 488 cm⁻¹ can be assigned to the host LDH structure (Zn-OH or Al-OH translation mode, or a combination of both[41]). The vibrational spectra of Zn,Al-Cp*MoO₃ indicate that the sample may contain minor amounts of carbonate and nitrate ions since a weak shoulder is observed in the IR spectrum at *ca.* 1365 cm⁻¹ (possibly due to $\nu_3(CO_3^{2-})$), and the Raman spectrum contains a weak band at 1042 cm⁻¹ (possibly due to $\nu_1(NO_3^-)$).
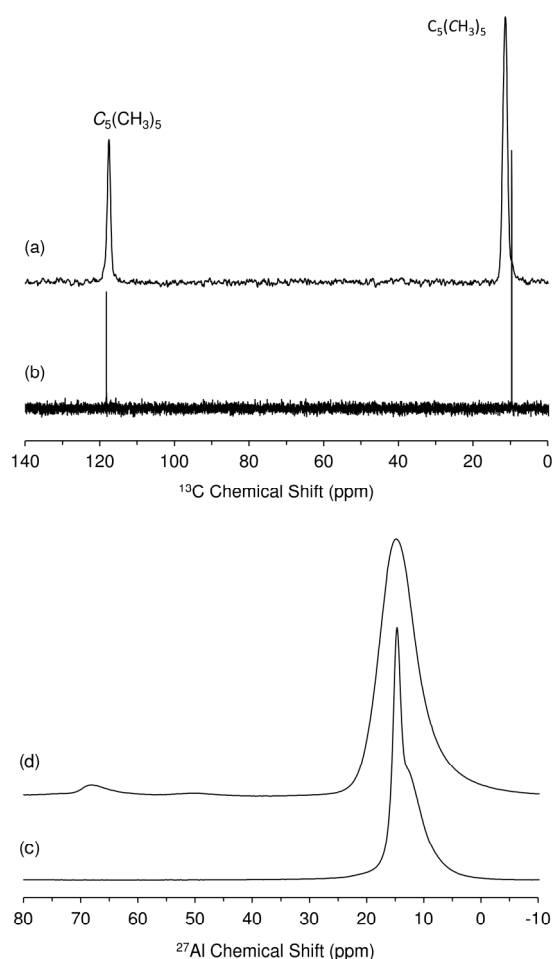
The ¹³C{¹H} CP MAS NMR spectrum of Zn,Al-Cp*MoO₃ (Figure 4) displays sharp signals at 11.3 ppm for the methyl groups of the Cp* ligand, and 117.5 ppm for the cyclopentadienyl carbon atoms. The latter resonance is unshifted when compared with that for Na[Cp*MoO₃] in D₂O, while the methyl signals are shifted downfield by 1.7 ppm. The ²⁷Al MAS NMR spectrum of Zn,Al-Cp*MoO₃ (Figure 4) is similar to those reported previously for Zn,Al and Mg,Al LDHs,[22,42-45] displaying a main peak at 14.8 ppm (Al1) and a broad shoulder at lower ppm (Al2), both assigned to octahedral Al environments. The presence of two distinct sites was confirmed in several studies by 3Q ²⁷Al MAS NMR.[22,42-44] The Al2 resonance is related to a site with a larger quadrupole coupling constant, corresponding to relatively distorted local Al environments, while Al1 has been attributed to more ordered and symmetric AlO_6 environments. For Mg,Al LDHs, Cadars *et al.* attributed the sharp peak to Al(Mg)₆ moieties (*i.e.*, the Al sites expected for an ideal ordered LDH framework with Mg/Al = 2), while the broad peak at lower ppm was assigned to less-symmetric Al(Mg)₅(Al) and Al(Mg)₄(Al)₂ environments associated with Al clustering and Al-O-Al linkages.[45] A similar assignment can be made for the two resonances observed in the spectra of Zn,Al LDHs. No resonance due to an Al-rich secondary phase was observed in the ²⁷Al MAS NMR spectrum of Zn,Al-Cp*MoO₃, indicating that the Al³⁺ cations were located exclusively within the layers.

The phase purity of the material Zn,Al-Cp*MoO₃ was further checked by SEM and elemental mapping by EDS (Figure 5). The morphology of the intercalated LDH consisted of aggregates of irregular sheet-like nanoparticles with sizes in the range 5-50 nm. Spatial elemental profiles showed a homogeneous distribution of Zn, Al and Mo across the particles. No evidence was found for secondary phases containing Zn (*e.g.* ZnO) and/or Al (*e.g.* Al₂O₃), in agreement with the PXRD and ²⁷Al MAS NMR data. EDS analyses gave an average Zn/Al molar ratio of 2.1 ± 0.1 and a Zn/Mo molar ratio of 2.5 ± 0.2.

Elemental (CHN) and thermogravimetric analyses were performed to establish the composition of Zn,Al-Cp*MoO₃. In the TGA curve (Figure 6), the first weight loss step of 9.4% from ambient temperature to 140 °C (with a derivative maximum (Dr_max) at 100 °C) corresponds to the removal of physisorbed and interlamellar water. No well-defined plateau is reached before the onset at *ca.* 140 °C of dehydroxylation, which extends up to 280 °C (Dr_max 180 °C, 15.1% mass loss) and is followed by two overlapping decomposition steps (Dr_max 370, 495 °C), leading to a final residual mass of 60.6% at 550 °C. The 15.1% mass loss in the range 140-280 °C has a contribution from the overlapping decomposition of the anion [Cp*MoO₃]⁻. For comparison, decomposition of the trioxido anion in Na[Cp*MoO₃]·2.5H₂O occurs abruptly above 150 °C after loss of water molecules, with a Dr_max value of 180 °C (Figure 6).

In a separate experiment, a portion of Zn,Al-Cp*MoO₃ was calcined under air at 550 °C for 8 h to give a MMO composite denoted calZn,Al-Cp*MoO₃. Bragg peaks due to ZnO (ICDD 04-007-9805) and α-ZnMoO₄ (ICDD 04-012-5025) were identifiable in the resultant PXRD pattern (Figure 1). To the best of our knowledge, the use of an intercalated LDH as a precursor to a MMO composite containing ZnMoO₄ as one of the components

Figure 4. (a) ¹³C{¹H} CP MAS NMR spectrum of Zn,Al-Cp*MoO₃, (b) solution ¹³C NMR spectrum of Na[Cp*MoO₃] (D₂O), (c) ²⁷Al MAS NMR spectrum of Zn,Al-Cp*MoO₃, and (d) ²⁷Al MAS NMR spectrum of calZn,Al-Cp*MoO₃.

has only been reported previously for heptamolybdate($Mo_7O_{24}^{6-}$)-intercalated Zn,Al materials.[46] Two broad diffraction peaks in the range 57-67° 2θ for calZn,Al-Cp*MoO$_3$ are tentatively assigned to $ZnAl_2O_4$ spinel (gahnite). The presence of this phase is supported by the ^{27}Al MAS NMR spectrum which matches literature data[47,48] for zinc aluminate spinels in showing one main broad peak at 15.0 ppm, assigned to octahedrally coordinated aluminium, and a much weaker broad peak at 68.2 ppm, assigned to tetrahedrally coordinated aluminium. The spectrum indicates a low degree of cation inversion, i.e. only a very low fraction of Al^{3+} cations occupy tetrahedral sites in the spinel structure. SEM images of calZn,Al-Cp*MoO$_3$ showed that the sheet-like morphology of the precursor nanoparticles had been lost upon calcination, consistent with a collapse of the lamellar structure (Figure 5). The elemental mapping images of the MMO showed a homogeneous distribution of Zn, Al and Mo, as expected for a well-dispersed ternary mixed phase as compared to individual and segregated oxides, for which no evidence was found.
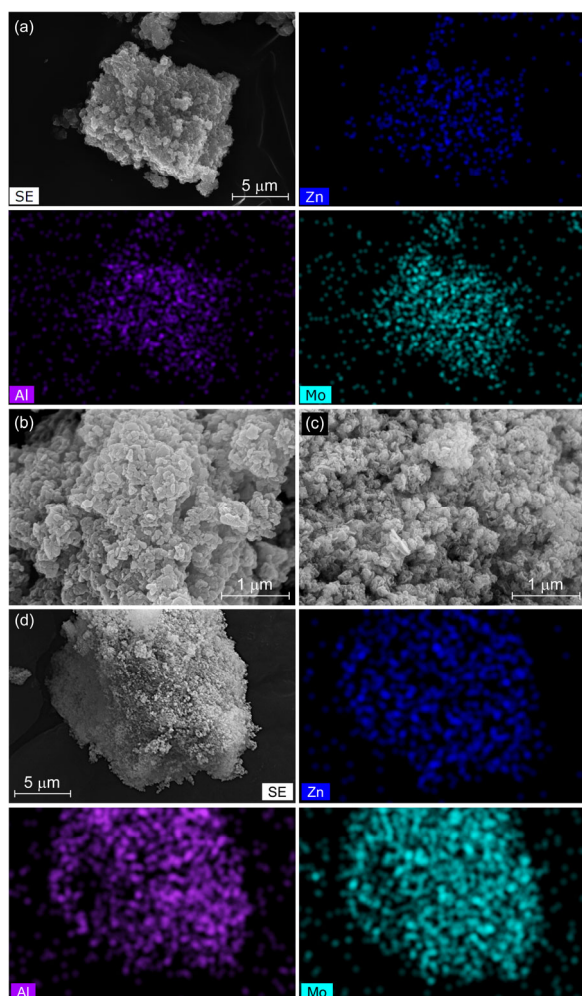
Figure 5. Representative SEM and corresponding EDS elemental mapping images of Zn,Al-Cp*MoO$_3$ (a, b) and calZn,Al-Cp*MoO$_3$ (c, d). Sample coating: (a) carbon, (b-d) gold/palladium.
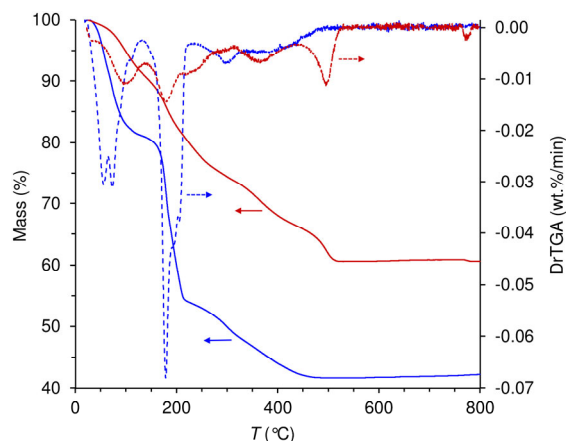
Figure 6. TGA (solid lines) and corresponding differential thermogravimetric (dashed lines) curves for Na[Cp*MoO$_3$]·2.5H$_2$O (blue) and Zn,Al-Cp*MoO$_3$ (red).

From the CHN, EDS and TGA analyses, together with the other characterization data, the formula Zn$_4$Al$_2$(OH)$_{12}$(Cp*MoO$_3$)$_{1.6}$(NO$_3$)$_{0.2}$(CO$_3$)$_{0.1}$·5.6H$_2$O is proposed for the material Zn,Al-Cp*MoO$_3$. It follows that the composition of the MMO calZn,Al-Cp*MoO$_3$ should be 1.4ZnO:1.6ZnMoO$_4$:ZnAl$_2$O$_4$, which fits precisely with the residual mass of 60.6% observed by TGA at 550 °C.

Catalytic studies

The complex Na[Cp*MoO$_3$]·2.5H$_2$O, the LDHs Zn,Al-NO$_3$ and Zn,Al-Cp*MoO$_3$, and the MMO calZn,Al-Cp*MoO$_3$ were screened as catalysts for the epoxidation of *cis*-cyclooctene (Cy) with TBHP as terminal oxidant, and α,α,α-trifluorotoluene (tft) as solvent (Table 1). The trioxido complex, as its sodium salt, is a sluggish catalyst for Cy epoxidation (60% conversion after 24 h at 70 °C, 100% selectivity towards the epoxide CyO). Under these conditions a blank reaction performed in the absence of Mo complex gave 11% Cy conversion. For the purpose of comparison, the two Cp*-Mo^{VI} complexes that are most closely related to the trioxido complex are the dioxido complex [Cp*MoO$_2$Cl] and the bimetallic complex [Cp*$_2$Mo$_2$O$_5$]; the latter can be considered as a complex of the type [Cp*MoO$_2$X] in which X is formally replaced by [Cp*MoO$_3$]$^-$. Like the trioxido complex, these two complexes display moderate catalytic activity for the epoxidation of Cy with TBHP/decane.[49,50] With the mononuclear dioxido complex, CyO yields were limited to 50-65% for reaction times between 4 and 24 h (1 mol% Mo, 2 equiv. TBHP, 55 °C).[49,50] A slightly improved long-term performance was observed for the dinuclear complex (87% CyO yield at 24 h).[50] The moderate catalytic performance of these Cp*-Mo^{VI} complexes can be attributed to various factors. For mononuclear [Cp*MoO$_2$Cl], the catalytically inactive peroxo complex [Cp*MoO(O$_2$)Cl] may be formed *in situ*,[51] and the original catalyst may suffer decomposition problems (involving loss of the Cp* ligand).[49] Investigations of the reaction of the dinuclear complex with TBHP/decane showed that oxidative

decomposition took place to give poorly active polyoxometalate ($[Mo_6O_{19}]^{2-}$) species.[52] For all Cp*-Mo^{VI} complexes, the electron-donating ability of the Cp* ligand may have a strong influence. Molybdenum-catalyzed epoxidation of olefins with hydroperoxides mechanistically involves an associative Lewis acid-base type reaction where the molybdenum species act as Lewis acids in the activation of the hydroperoxide oxidant, which is necessary for the epoxidation reaction to occur.[53,54] The strong electron donating ability of the Cp* ligand may reduce the Lewis-acidity of the complexes and therefore negatively impact the catalytic activity. A similar argument has been put forward to explain the lack of activity of the rhenium complex [Cp*ReO$_3$] for oxidation reactions.[55]

Table 1. *cis*-Cyclooctene epoxidation with TBHP.

Compound	T (°C)	Solvent	Conversion at 24 h (%)[a]
Zn,Al-NO$_3$	70	tft	6
Na[Cp*MoO$_3$]·2.5H$_2$O	70	tft	60
Zn,Al-Cp*MoO$_3$	70	tft	15
calZn,Al-Cp*MoO$_3$	70	tft	69/77/65[b]
Zn,Al-Cp*MoO$_3$	85	No solvent	51
calZn,Al-Cp*MoO$_3$	85	No solvent	100

[a] Cyclooctene oxide was always the only product formed. [b] Conversion in three consecutive 24 h-batch runs.

The material Zn,Al-Cp*MoO$_3$ displayed poor activity for Cy epoxidation with TBHP/decane (15% conversion after 24 h at 70 °C, 100% selectivity towards CyO). This conversion is only slightly superior to that measured for the nitrate-form LDH Zn,Al-NO$_3$, which led to 6% conversion after 24 h. Iodometric titration to quantify TBHP in the reaction mixture after a 24 h run with Zn,Al-Cp*MoO$_3$ indicated no measurable non-productive decomposition of the oxidant to molecular oxygen and *tert*-butanol. Hence, the intercalated LDH did not exhibit competing catalase activity. Performing the epoxidation reaction at a slightly higher temperature of 85 °C in the absence of cosolvent led to significantly higher activity (31% conversion after 6 h, 51% conversion after 24 h).

The low catalytic activity of Zn,Al-Cp*MoO$_3$ can be attributed to two main factors: the low intrinsic activity of the intercalated trioxido complex, and the inaccessibility of the active sites due to the efficient close-packing of intercalated guest molecules. The latter drawback is common to many LDH intercalation catalysts prepared by the immobilization of molecular catalysts.[56] Of all the reported intercalation catalysts, the one most similar to Zn,Al-Cp*MoO$_3$ is the previously mentioned Zn,Al LDH intercalated by the tricarbonyl complex [CpMo(CO)$_3$CH$_2$COO$^-$].[29] Cyclopentadienyl molybdenum tricarbonyl complexes can be used directly as catalyst precursors in olefin epoxidation with TBHP/decane, being oxidized *in situ* to active Mo^{VI} catalysts such as the dioxido

complexes [CpMoO$_2$X]. The intercalated tricarbonyl complex led to a respectable CyO yield of 97% after 24 h at 55 °C (1 mol% Mo).[29] However, catalytic performance for the recovered catalyst decreased in recycling runs.

One of the most successful implementations of LDHs in catalysis involves their controlled thermal decomposition to generate well-dispersed, porous MMO materials.[56] The composition of the MMO can be tuned as desired by varying the identity and molar ratio of M^{2+} and M^{3+} cations in the LDH layers. Calcining LDHs intercalated with metal-containing anions allows the preparation of MMOs containing metals that cannot be incorporated within the hydroxide layers. For this reason a Zn-Al-Mo MMO was prepared from Zn,Al-Cp*MoO$_3$ and tested as a catalyst for Cy epoxidation. The material calZn,Al-Cp*MoO$_3$ was far more active than Zn,Al-Cp*MoO$_3$, leading to 69% conversion after 24 h at 70 °C (Table 1). This level of conversion was maintained in a further two consecutive 24 h batch runs using the recovered catalyst. FT-IR and PXRD data for the recovered catalysts showed no major changes in relation to the data for the as-prepared MMO (not shown here). When the reaction was performed at 85 °C in the absence of cosolvent, complete conversion and quantitative epoxide yield were achieved within 24 h.

Conclusions

The direct coprecipitation technique is already known to allow the intercalation of organic anions, inorganic anions and metal coordination compounds into layered double hydroxides. The present work shows that, using this approach under mild conditions, the complex [Cp*MoO$_3$]$^-$ can be intercalated to produce a new material with an interlayer distance of 17.1 Å, as determined by PXRD. The extensive characterization of the material indicates that upon intercalation the Cp* ligands of the half-sandwich complex are retained and exert a decisive structure-directing effect on the organization of the molecular array. The self-assembly process is thus driven by π-stacking interactions in synergy with the electrostatic interaction between the host lattice and guest molecules, and hydrogen-bonding interactions between the oxido ligands of the trioxido complex and the layer hydroxyl groups. To the best of our knowledge, this is the first report of the intercalation of an intrinsically anionic metallocene or half-sandwich complex in an LDH. The synthetic approach is expected to be suitable for other water-soluble anionic complexes, providing new opportunities for materials design by using LDHs as templates for supramolecular organometallic structures.

Experimental Section

Materials and methods: The chemicals 1,2,3,4,5-pentamethylcyclopentadiene (94%, Alfa-Aesar), sodium amide, hexane (99%) Mo(CO)$_6$, anhydrous tetrahydrofuran (99%), 70% TBHP in water, Zn(NO$_3$)$_2$·6H$_2$O (Fluka), Al(NO$_3$)$_3$·9H$_2$O (Riedel-de-Haën), 1 M NaOH, sodium carbonate (José M. Vaz Pereira), *cis*-cyclooctene (95%, Alfa Aesar), 5.5 M TBHP in decane, α,α,α-trifluorotoluene (>99%), diethyl ether (99.8%), pentane (95%, Carlo Erba), and undecane (> 99%) were

purchased from Sigma-Aldrich unless otherwise stated, and used as received. A nitrate-form Zn,Al LDH (denoted Zn,Al-NO$_3$) with the composition Zn$_4$Al$_2$(OH)$_{12}$(NO$_3$)$_2$·2.5H$_2$O was prepared by using the standard method of coprecipitation of the Zn^{2+} and Al^{3+} hydroxides (initial Zn^{2+}/Al^{3+} molar ratio in solution = 2) in the presence of nitrate ions at constant pH (7.5–8) under nitrogen, followed by aging of the gel at 80 °C for 20 h.[57,58] Unless otherwise stated, all preparations and manipulations were carried out using Schlenk techniques under a nitrogen atmosphere.

Physical measurements: Microanalyses for C, H and N were carried out at the Department of Chemistry, University of Aveiro, with a Truspec Micro CHNS 630-200-200 elemental analyzer. SEM images, EDS analyses and elemental mapping images were obtained with either a Hitachi SU-70 microscope equipped with a Bruker Quantax 400 detector operating at 15 kV, or a Hitachi S4100 microscope operating at 25 kV. Samples were prepared by deposition on aluminium sample holders followed by sputter-coating with carbon or gold/palladium. PXRD data were collected at ambient temperature using a PANalytical Empyrean instrument equipped with a PIXcel 1D detector set at 240 mm from the sample. Cu-K$_{\alpha1,2}$ X-radiation (λ_1 = 1.540598 Å; λ_2 = 1.544426 Å) filtered with a nickel foil was used along with a standard transmission sample holder. Working operating conditions for the X-ray tube: 45 kV and 40 mA. Intensity data were collected in continuous mode in the *ca.* 3.0-70° 2θ range. Samples were step-scanned in 0.02° 2θ steps with a counting time of 100 s per step. Phase identification was performed with the HighScore Plus software package (PANalytical) and the ICDD PDF-2 database. TGA was performed using a Shimadzu TGA-50 system at a heating rate of 5 °C min^{-1} under air. FT-IR spectra (KBr pellets) were obtained using a Mattson-7000 spectrophotometer. Raman spectra were recorded on a Bruker RFS100/S FT instrument (Nd:YAG laser, 1064 nm excitation, InGaAs detector). ^{1}H and ^{13}C NMR spectra in solution were measured on a Bruker CXP 300 instrument. Solid-state ^{13}C{^{1}H} CP MAS NMR spectra were recorded at 100 MHz on a Bruker Avance 400 spectrometer with 3.2 μs ^{1}H 90° pulses, 3.5 ms contact time, spinning rates of 12 kHz, and 5 s recycle delays. Chemicals shifts are quoted in ppm relative to TMS. ^{27}Al MAS NMR spectra were acquired using short and powerful radio-frequency pulses of 0.27 μs, a spinning rate of 15 kHz and a recycle delay of 0.5 s. Chemicals shifts are quoted in ppm relative to Al(H$_2$O)$_6$$^{3+}$.

Synthesis of Na[Cp*MoO$_3$]·nH$_2$O: Minor modifications were made to the synthetic procedure described by Dinoi *et al.*[34] Cp*H (2.30 mL, 14.7 mmol) was added to a suspension of sodium amide (0.57 g, 14.7 mmol) in THF (30 mL). The mixture was refluxed for 24 h at 90 °C. After this time the mother liquor was filtered off, evaporated to dryness, and the solid residue (NaCp*) washed with hexane (2 × 20 mL). A solution of Mo(CO)$_6$ (3.88 g, 14.7 mmol) in THF (60 mL) was then added, and the mixture was refluxed overnight. The resultant dark brown solution was cooled to room temperature and a previously degassed solution of 0.8 M NaOH (93 mL) was slowly added. Dropwise addition of 70% aq. TBHP (12 mL, 88.2 mmol) to the latter solution resulted in a color change from dark brown to red with vigorous gas evolution. The solution was stirred for 72 h at room temperature. Excess peroxide was destroyed by adding MnO$_2$ to the yellow solution followed by stirring at room temperature. The solution was filtered off, evaporated to dryness under reduced pressure, and the resultant yellow solid was extracted with hot THF (5 × 20 mL). All the THF fractions were combined, and then the solution was concentrated before storing overnight in a fridge. A yellow precipitate of Na[Cp*MoO$_3$] formed and was isolated by filtration (0.90 g, 18%). Anal. Calcd for C$_{10}$H$_{20}$MoNaO$_{5.5}$ (Na[Cp*MoO$_3$]·2.5H$_2$O) (347.19): C, 34.59; H, 5.81. Found: C, 34.71; H, 5.39. Selected FT-IR (cm^{-1}) $\tilde{v}$ = 3380 (br), 2971 (w), 2915 (m), 2858 (w), 1642 (br), 1599 (br), 864 (vs, ν(Mo=O)), 816 (vs, ν(Mo=O)), 797 (vs, ν(Mo=O)); FT-Raman (cm^{-1}) $\tilde{v}$ = 3379 (br), 2978 (sh), 2911 (vs), 1465 (m), 1431 (m), 1407 (m), 1383 (m), 1166 (w),

1062 (w), 1027 (w), 869 (vs), 815 (m), 797 (m), 626 (w), 595 (s), 548 (m), 415 (m), 333 (m), 289 (m), 155 (s); ^{1}H NMR (300 MHz, D$_2$O, 298 K) δ = 1.90 (s, 15H, C$_5$Me$_5$); ^{13}C NMR (75 MHz, D$_2$O, 298 K) δ = 118.2 (s, C$_5$Me$_5$), 9.6 (s, C$_5$Me$_5$).

Synthesis of Zn,Al-Cp*MoO$_3$: The LDH was prepared by a co-precipitation method. The reaction was carried out under nitrogen using distilled deionized (DD) water which was freshly decarbonated prior to use by vigorously boiling for 15 min. A solution of Na[Cp*MoO$_3$]·2.5H$_2$O (0.60 g, 1.7 mmol) in DD water (40 mL) was purged with nitrogen for 1 h and the pH was adjusted to 7.25±0.25. A solution of Zn(NO$_3$)$_2$·6H$_2$O (0.59 g, 2 mmol) and Al(NO$_3$)$_3$·9H$_2$O (0.37 g, 1 mmol) in DD water (40 mL) was added dropwise, and the pH of the mixture was continuously maintained between 7.5 and 8 by dropwise addition of 0.2 M NaOH. After the addition was complete, the gel-like slurry was aged at 65 °C for 20 h. The resultant pale yellow solid was filtered, washed several times with DD water, and finally vacuum-dried. Anal. Calcd for Zn$_4$Al$_2$(OH)$_{12}$(Cp*MoO$_3$)$_{1.6}$(NO$_3$)$_{0.2}$(CO$_3$)$_{0.1}$·5.6H$_2$O (1085.6): C, 17.81; H, 4.38; N, 0.26. Found: C, 17.50; H, 4.38; N, 0.25. EDS gave an average Zn/Al ratio of 2.1 ± 0.1 and an average Zn/Mo ratio of 2.5 ± 0.2. TGA showed a mass loss of 9.4% up to 140 °C (calcd, for loss 5.6H$_2$O: 9.3%), and a residual mass of 60.6% at 550 °C (calcd, for Zn$_4$Al$_2$Mo$_{1.6}$O$_{11.8}$: 60.6%). FT-IR (cm^{-1}) $\tilde{v}$ = 3456 (br), 2912 (m), 2856 (w), 1635 (m), 1496 (w), 1384 (w), 1360 (sh), 1261 (w), 1068 (w), 1026 (m), 864 (vs), 812 (sh), 795 (vs), 623 (s), 555 (m), 424 (s); FT-Raman (cm^{-1}) $\tilde{v}$ = 3400 (br), 2956 (m), 2911 (s), 2859 (sh), 1465 (m), 1435 (s), 1387 (m), 1366 (w), 1167 (w), 1069 (w), 1042 (w), 1028 (w), 870 (vs), 810 (m), 789 (m), 598 (s), 549 (m), 488 (w), 417 (m), 332 (m), 287 (m), 195 (s), 161 (s); ^{13}C{^{1}H} CP MAS NMR δ = 117.5 (C$_5$Me$_5$), 11.3 (C$_5$Me$_5$); ^{27}Al MAS NMR δ = 14.8 ppm.

Catalytic tests: The epoxidation reactions were carried out with magnetic stirring (1000 rpm) in 12 mL borosilicate batch reactors equipped with a PTFE valve for sampling. The reactor containing the catalyst, substrate and solvent (when used) was immersed in a temperature-controlled oil bath for 10 min, after which TBHP in decane (preheated at 70 or 85 °C) was added to give an initial Mo:substrate:oxidant molar ratio of 1:100:200; the reaction time was counted from this instant. The evolution of the reaction was monitored by regular sampling and gas chromatographic analysis using an Agilent 7820AGC, equipped with a HP-5 capillary column (30 m × 0.320 mm × 0.25 μm) and a flame ionization detector (H$_2$ as carrier gas, undecane as internal standard). For product identification selected samples were analyzed by GC-MS using a Trace GC 2000 Series (Thermo Quest CE Instruments GC) - DSQ II (Thermo Scientific instrument), with He as the carrier gas.

Iodometric titration was carried out for a 24 h batch run. After the catalytic run, the liquid phase was separated from the reaction mixture using a 0.20 μm PTFE membrane.

For catalyst reuse, the solid was separated by centrifugation, washed with pentane and diethyl ether, dried at room temperature overnight and finally vacuum-dried (*ca.* 4 bar) at 60 °C for 1 h.

Acknowledgments

[1]   A. Lerf, *Dalton Trans.* **2014**, *43*, 10276-10291.
[2]   R. Schöllhorn, *Chem. Mater.* **1996**, *8*, 1747-1757.
[3]   M. Ogawa, K. Kuroda, *Chem. Rev.* **1995**, *95*, 399-438.
[4]   J. Wan, S. D. Lacey, J. Dai, W. Bao, M. S. Fuhrer, L. Hu, *Chem. Soc. Rev.* **2016**, *45*, 6742-6765.
[5]   D. O'Hare, *New. J. Chem.* **1994**, *18*, 989-998.
[6]   M. B. Dines, *Science* **1975**, *188*, 1210-1211.
[7]   H.-V. Wong, R. Millett, J. S. O. Evans, S. Barlow, D. O'Hare, *Chem. Mater.* **1995**, *7*, 210-214.
[8]   A. Ibarz, E. Ruiz, S. Alvarez, *J. Chem. Soc., Dalton Trans.* **2000**, 1463-1467.
[9]   E.-W. Scheidt, M. Herzinger, A. Fischer, D. Schmitz, J. Reiners, F. Mayr, F. Loder, M. Baenitz, W. Scherer, *J. Phys.: Condens. Matter* **2015**, *27*, 155701.
[10]   Z. Li, Y. Zhao, K. Mu, H. Shan, Y. Guo, J. Wu, Y. Su, Q. Wu, Z. Sun, A. Zhao, X. Cui, C. Wu, Y. Xie, *J. Am. Chem. Soc.* **2017**, *139*, 16398-16404.
[11]   T. R. Halbert, D. C.Johnston, L. E. McCandlish, A. H. Thompson, J. C. Scanlon, J. A. Dumesic, *Physica B+C* **1980**, *99*, 128-132.
[12]   R. Clement, M. L. H. Green, *J. Chem. Soc., Dalton Trans.* **1979**, 1566-1568.
[13]   A. M. Fogg, V. M. Green, D. O'Hare, *Chem. Mater.* **1999**, *11*, 216-217.
[14]   S. J. Mason, L. M. Bull, Clare P. Grey, Stephen J. Heyes, D. O'Hare, *J. Mater. Chem.* **1992**, *2*, 1189-1194.
[15]   J. W. Johnson, *J. Chem. Soc., Chem. Commun.* **1980**, 263-265.
[16]   M. B. Santiago, M. Declet-Flores, A. Díaz, M. M. Vélez, M. Z. Bosques, Y. Sanakis, J. L. Colón, *Langmuir* **2007**, *23*, 7810-7817.
[17]   B. Casañas-Montes, A. Díaz, C. Barbosa, C. Ramos, C. Collazo, E. Meléndez, C. Queffelec, F. Fayon, A. Clearfield, B. Bujoli, J. L. Colón, *J. Organomet. Chem.* **2015**, *791*, 34-40.
[18]   S. Okuno, G. Matsubayashi, *J. Chem. Soc., Dalton Trans.* **1992**, 2441-2444.
[19]   Y. Zhu, Y. Qian, Z. Ju, L. Peng, G. Yu, *Nano Lett.* **2018**, *18*, 6071-6075.
[20]   J. Tudor, L. Willington, D. O'Hare, B. Royan, *Chem. Commun.* **1996**, 2031-2032.
[21]   W. R. Mariott, E. Y.-X. Chen, *J. Am. Chem. Soc.* **2003**, *125*, 15726-15727.
[22]   S. Gago, M. Pillinger, T. M. Santos, J. Rocha, I. S. Gonçalves, *Eur. J. Inorg. Chem.* **2004**, 1389-1395.
[23]   M. Colombari, B. Ballarin, I. Carpani, L. Guadagnini, A. Mignani, E. Scavetta, D. Tonelli, *Electroanalysis* **2007**, *19*, 2321-2327.
[24]   S. Morlat-Thérias, C. Mousty, P. Palvadeau, P. Molinié, P. Léone, J. Rouxel, C. Taviot-Guého, A. Ennaqui, A. de Roy, J. P. Besse, *J. Solid State Chem.* **1999**, *144*, 143-151.
[25]   S. Therias, B. Lacroix, B. Schöllhorn, C. Mousty, P. Palvadeau, *J. Electroanal. Chem.* **1998**, *454*, 91-97.
[26]   P. Wang, G. Zhu, *Electrochem. Commun.* **2002**, *4*, 36-40.
[27]   C. Mousty, C. Forano, S. Fleutot, J.-C. Dupin, *Electroanalysis* **2009**, *21*, 399-408.

[28]   D. S. Glueck, A. R. Brough, P. Mountford, M. L. H. Green, *Inorg. Chem.* **1993**, *32*, 1893-1902.
[29]   A. C. Gomes, S. M. Bruno, M. Abrantes, C. I. R. Magalhães, I. S. Gonçalves, A. A. Valente, M. Pillinger, *J. Organomet. Chem.* **2014**, *760*, 205-211.
[30]   D.G. Evans, R.C.T. Slade, Structural aspects of layered double hydroxides, in *Layered Double Hydroxides* (Eds. X. Duan, D.G. Evans), *Structure and Bonding*, vol. 119, Springer, Berlin, Heidelberg, **2006**, pp. 1-87.
[31]   S. P. Newman, W. Jones, *New J. Chem.* **1998**, *22*, 105-115.
[32]   V. Rives, M. A. Ulibarri, *Coord. Chem. Rev.* **1999**, *181*, 61-120.
[33]   C. Taviot-Guého, V. Prévot, C. Forano, G. Renaudin, C. Mousty, F. Leroux, *Adv. Funct. Mater.* **2018**, *28*, 1703868.
[34]   C. Dinoi, G. Taban, P. Sözen, F. Demirhan, J.-C. Daran, R. Poli, *J. Organomet. Chem.* **2007**, *692*, 3743-3749.
[35]   A. C. Gomes, S. M. Bruno, A. A. Valente, I. S. Gonçalves, M. Pillinger, *J. Organomet. Chem.* **2013**, *744*, 53-59.
[36]   P. Beaudot, M. E. De Roy, J. P. Besse, *J. Solid State Chem.* **2001**, *161*, 332-340.
[37]   M. del Arco, S. Gutiérrez, C. Martín, V. Rives, *Inorg. Chem.* **2003**, *42*, 4232-4240.
[38]   K. Cermelj, K. Ruengkajorn, J.-C. Buffet, D. O'Hare, *J. Energy Chem.* **2019**, *35*, 88-94.
[39]   M. Vucelic, G. D. Moggridge, W. Jones, *J. Phys. Chem.* **1995**, *99*, 8328-8337.
[40]   M. S. Rau, C. M. Kretz, G. L. Geoffroy, A. L. Rheingold, *Organometallics* **1993**, *12*, 3447-3460.
[41]   J. T. Kloprogge, L. Hickey, R. L. Frost, *J. Solid State Chem.* **2004**, *177*, 4047-4057.
[42]   J. Rocha, M. del Arco, V. Rives, M. A. Ulibarri, *J. Mater. Chem.* **1999**, *9*, 2499−2503.
[43]   P. Benito, F. M. Labajos, L. Mafra, J. Rocha, V. Rives, *J. Solid State Chem.* **2009**, *182*, 18-26.
[44]   A. Vyalikh, F. R. Costa, U. Wagenknecht, G. Heinrich, D. Massiot, U. Scheler, *J. Phys. Chem. C* **2009**, *113*, 21308-21313.
[45]   S. Cadars, G. Layrac, C. Gérardin, M. Deschamps, J. R. Yates, D. Tichit, D. Massiot, *Chem. Mater.* **2011**, *23*, 2821-2831.
[46]   D. Carriazo, C. Domingo, C. Martín, V. Rives, *Inorg. Chem.* **2006**, *45*, 1243-1251.
[47]   V. Šepelák, I. Bergmann, S. Indris, A. Feldhoff, H. Hahn, K. D. Becker, C. P. Grey, P. Heitjans, *J. Mater. Chem.* **2011**, *21*, 8332-8337.
[48]   M.-Y. Guan, D.-M. Xu, Y.-F. Song, Y. Guo, *Sens. Actuators B: Chem.* **2013**, *188*, 1148-1154.
[49]   M. Abrantes, A. M. Santos, J. Mink, F. E. Kühn, C. C. Romão, *Organometallics* **2003**, *22*, 2112-2118.
[50]   A. M. Martins, C. C. Romão, M. Abrantes, M. C. Azevedo, J. Cui, A. R. Dias, M. T. Duarte, M. A. Lemos, T. Lourenço, R. Poli, *Organometallics* **2005**, *24*, 2582-2589.
[51]   M. K. Trost, R. G. Bergman, *Organometallics* **1991**, *10*, 1172-1178.
[52]   C. Bhaumik, E. Manoury, J.-C. Daran, P. Sözen-Aktaş, F. Demirhan, R. Poli, *J. Organomet. Chem.* **2014**, *760*, 115-123.
[53]   P. J. Costa, M. J. Calhorda, F. E. Kühn, *Organometallics* **2010**, *29*, 303-311.
[54]   A. Comas-Rives, A. Lledós, R. Poli, *Chem Eur. J.* **2010**, *16*, 2147-2158.
[55]   M. Högerl, F. E. Kühn, *Z. Anorg. Allg. Chem.* **2008**, *634*, 1444-1447.
[56]   G. Fan, F. Li, D. G. Evans, X. Duan, *Chem. Soc. Rev.* **2014**, *43*, 7040-7066.
[57]   A. C. Gomes, S. M. Bruno, C. A. Gamelas, A. A. Valente, M. Abrantes, I. S. Gonçalves, C. C. Romão, M. Pillinger, *Dalton Trans.* **2013**, *42*, 8231-8240.
[58]   A. L. Costa, A. C. Gomes, M. Pillinger, I. S. Gonçalves, J. Pina, J. S. Seixas de Melo, *ChemPhysChem* **2017**, *18*, 564-575.

Entry for the Table of Contents

FULL PAPER

A molecular array of [Cp*MoO₃]⁻ anions, organized into a bilayer via Cp*⋯Cp* interactions, has been sandwiched between the layers of a layered double hydroxide (LDH) host by a direct coprecipitation method. The intercalated LDH and the mixed metal oxide obtained after its calcination were characterized and examined as catalysts for the epoxidation of *cis*-cyclooctene.
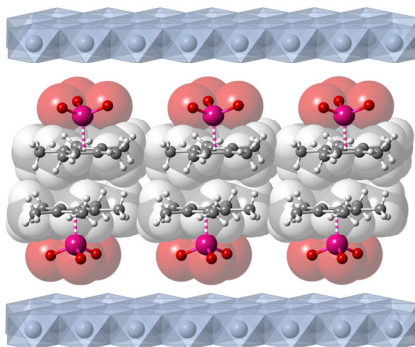
Organometallic Intercalates

Ana C. Gomes, Patrícia Neves, Sandra Gago, Anabela A. Valente,* Isabel S. Gonçalves, and Martyn Pillinger*

Page No. – Page No.

Intercalation of (η^5-pentamethylcyclopentadienyl)trioxo-molybdenum(VI) in a layered double hydroxide